Western University

Scholarship@Western

Bone and Joint Institute

2-29-2016

A rigid body model for the assessment of glenohumeral joint mechanics: Influence of osseous defects on range of motion and dislocation

Mark F. Welsh
Hand and Upper Limb Centre

Ryan T. Willing
Hand and Upper Limb Centre

Joshua W. Giles
Hand and Upper Limb Centre

George S. Athwal
Hand and Upper Limb Centre

James A. Johnson
Hand and Upper Limb Centre

ABSTRACT

The purpose of this study was to employ subject-specific computer models to evaluate the interaction of glenohumeral range-of-motion and Hill-Sachs humeral head bone defect size on engagement and shoulder dislocation. We hypothesized that the rate of engagement would increase as defect size increased, and that greater shoulder ROM would engage smaller defects. Three dimensional computer models of twelve shoulders were created. For each shoulder, additional models were created with simulated Hill-Sachs defects of varying severities (XS=15%, S=22.5%, M=30%, L=37.5%, XL=45% and XXL=52.5% of the humeral head diameter, respectively). Rotational motion simulations without translation were conducted. The simulations ended if the defect engaged the anterior glenoid rim with resultant dislocation. The results showed that the rate of engagement was significantly different between defect sizes ($0.001<p<0.032$). Defect engagement occurred for all specimens when defects size XL and XXL were simulated. Size M or L defects engaged in some (but not all) specimens. Defect engagement occurred at mean horizontal extension angles of -23.6±9.3°, -17.9±10.8°, -4.5±9.0°, and +6.4±8.8° for M, L, XL, and XXL defect sizes, respectively. Differences in engagement angle between defect sizes were significant for all comparisons ($p<0.001$). The model showed that XS and S size defects do not engage when only rotational motions are considered. Since engagement of XS and S size Hill-Sachs defects is believed to occur clinically, we suspect that some amount of joint translation may be occurring, causing these defects to engage. Therefore, further studies on clinical pre-operative joint laxity and ROM may enable the prediction of engagement.

KEYWORDS: Hill-Sachs; instability; shoulder; dislocation, multibody models

A Rigid Body Model for the Assessment of Glenohumeral Joint Mechanics: Influence of Osseous Defects on Range of Motion and Dislocation

INTRODUCTION

Humeral head defects are associated with glenohumeral joint dislocation and recurrent instability. Hill and Sachs (Hill and Sachs 1940) were the first to report these defects as being associated with shoulder instability. These defects, now referred to as Hill-Sachs defects (HSD), occur when the humerus dislocates anteriorly, causing an impression fracture on the posterosuperior humeral head as it impacts against the denser bone of the anterior glenoid rim. This defect has been reported in 65-80% of initial dislocations, and close to 100% of cases with recurrent dislocation (Calandra et al. 1989, Degen et al. 2013, Kaar et al. 2010, Taylor and Arciero 1997).

Several methods have been described for treating shoulder instability with associated HSDs including benign neglect, remplissage, allograft reconstruction, osteochondral transfer, humeroplasty, partial resurfacing arthroplasty, humeral osteotomy and hemiarthroplasty (Boileau et al. 2007, Boileau et al. 2006, Burkhart and Danaceau 2000, Burkhart and De Beer 2000, Chen et al. 2005, Giles et al. 2011, Kropf and Sekiya 2007, Re et al. 2006). These operative procedures vary in the techniques used to address the defect to eliminate defect-glenoid interaction. For example, the remplissage fills the defect with soft tissue, while allograft reconstruction, osteochondral transfer and humeroplasty use bone. Hemiarthroplasty and partial resurfacing reconstructions use metallic implants to fill the defect. In the case of HSDs, the treatment method may vary based on the properties of the defect and patient factors. Selecting the most appropriate technique is not always readily apparent, as the literature remains incomplete in examining the defect state and its interaction with the glenoid. There is also little consensus on the size of defect that will cause recurrent instability, as well as the joint position or type of movement that may cause defect engagement. Clinically, engagement occurs when the leading edge of the humeral articular defect moves anterior to the anterior glenoid rim, causing medialization of the humeral head on the glenoid, and resultant joint dislocation (Miniaci A, 2004). A study by Sekiya et al. (2009) suggests that defects as small as 12.5% of humeral head diameter may have biomechanical implications on glenohumeral stability, while a more recent study by Sekiya et al. (2012) argues that isolated defects that are less than 25.0% of humeral head width may not cause recurrent engagement. Studies by Kaar et al. (2010) and Walia et al. (2013) examined the effect of HSD sizes in different positions of abduction and external rotation, quantifying joint stability by the anterior translational distance before dislocation. These respective in-vitro and in-silico studies showed an inverse relationship between defect size and humeral translational distance before the onset of instability; however, they chose not to investigate the effects of isolated rotational movements, such as horizontal extension, on engagement and instability. This motion is clinically relevant, as it is more indicative of the manner that patients typically report recurrent dislocations(Taylor and Arciero, 1997), opposed to an incident occurring with an anteriorly directed force. Furthermore, surgeons may intra-operatively elect to place the humeral head into abduction and external rotation before horizontally extending the humerus to inspect defect engagement (Burkhart and De Beer, 2000). The literature remains uninformed on the influence of isolated rotation, thus supporting the need for further information regarding the effects of glenohumeral ROM on defect engagement and instability.

The purpose of this study was to employ 3D computer models to quantify the effects of humeral extension range of motion on HSD engagement. The influence of HSD size on the rate of engagement among twelve cadaveric shoulders and the glenohumeral joint angle at engagement was evaluated to determine a relationship between these variables. A computer model was selected to examine a broad range of conditions that could be calculated with a high level of repeatability, conforming to similar practice by Walia et al. (2013). We hypothesized that the rate of engagement would increase as HSD size increased, and additionally, simulations with greater degrees of shoulder range of motion (horizontal extension) would engage smaller defects.

METHODS

Specimen Modelling & Simulation Construction

Twelve unpaired male cadaveric shoulders (mean age: 65 years; age range: 21-77) were evaluated. Specimens were screened for exclusion criteria including osteoarthritis, trauma or previous surgery prior to model creation. CT scans with a slice thickness of 0.625mm and average pixel size of 0.592mm were used to create 3D models of the scapula and humerus via threshold-based segmentation (HU > 226) using Mimics 15.0 software (Materialise, Ann Arbor, MI). These models were wrapped, smoothed, and decimated to minimize staircase artifacts. The models were imported into the SolidWorks Motion Study software package (Dassault Systèmes SolidWorks Corp, Waltham, MA) and were converted into solid CAD geometries for analysis. An assembly was created with the humerus and scapula originally oriented in the neutral position (0° axial rotation, 0° abduction).

The model was designed to evaluate the effect of a HSD on glenohumeral movement in the position of abduction and external rotation, which is clinically associated with HSD engagement and called the 'apprehension position' due to a patient's sense of joint instability. Utilizing a standard 2:1 ratio of glenohumeral to scapulothoracic joint motion as described by McQuade et al. (McQuade and Smidt 1998), the scapula model was placed in the 30° abduction, the humerus model was placed in 60° of glenohumeral abduction in the scapular plane (scaption) and 60° external rotation, clinically referred to as the position of apprehension for shoulder instability (Fig. 1A). In this position, the orientation of the HSD was determined as defined by Sekiya et al.

(2009) and Yamamoto et al. (2007). To create the defect, a line was drawn on the humeral head parallel to the anterior glenoid rim (Fig. 1B), which represented the orientation of a defect on the humeral head caused by dislocation with the joint in the position of apprehension (Fig. 1A). The diameter of the humeral head perpendicular to this line was measured. HSDs of varying size were then created as a percentage of this diameter. The test conditions included an intact humeral head and HSD sizes of 15.0%, 22.5%, 30.0%, 37.5%, 45.0%, and 52.5% of the humeral head diameter. These defect sizes are herein referred to as extra-small (XS), small (S), medium (M), large (L), extra-large (XL), and extra-extra-large (XXL), respectively. The humeral head posterior and superior to the Hill-Sachs orientation line was removed for all defect sizes with material removed down to the articular margin thus creating a wedge shaped defect with a right angle at its base (Fig. 1C).

A series of points on the glenoid rim of the scapula model were used to create a plane of best fit oriented parallel to the glenoid face. A glenoid coordinate system was also created, with the origin within this best-fit plane, and located at the intersection of the axes measuring maximum glenoid superior/inferior length and anterior/posterior width (Fig. 2). Humeral head medial/lateral translation was measured as the distance from the center of the humeral head to the glenoid plane, measured along the lateral direction of the glenoid coordinate system. This distance was compared between intact and defect humeral head conditions. The approximate centre of the humeral head was calculated using a sphere-fit algorithm. As the purpose of the study was to determine the occurrence of humeral head engagement on the glenoid due to isolated humeral rotation, the humerus was restricted from translating in the anterior/posterior and superior/inferior directions once it was initially centered with respect to the glenoid. However, translations were permitted in the medial/lateral direction, as these are required to permit the HSDs to engage the glenoid rim.

Simulation Protocol

The scapula and humerus bone models were defined to be non-deformable rigid bodies. Motions were calculated using the default Gear Stiff (GSTIFF) integrator. Contact was modelled between the bones using an impact (penalty regularisation method) algorithm, and a high contact stiffness (100,000 N/mm) was chosen to eliminate penetration between the bone surfaces. As a compliant structure, cartilage was omitted in this rigid body model. The starting position of the shoulder for all simulations was 90° of abduction (Fig. 3A) – which was comprised of 60° of glenohumeral abduction and 30° of scapular elevation (i.e. a 2:1 scapulothoracic contribution) – in the sagittal plane with the humerus externally rotated by 60° (Fig. 3B). These rotations follow a YXY concept from the ISB recommendations by Wu et al. (2005), while mechanically defining the rotations in SolidWorks Motion Study software. Abduction beginning in the sagittal plane was chosen to account for testing scenarios where the largest Hill-Sachs defects could potentially engage before the humerus extended to the commonly described clinical position of apprehension in the scapular plane. As such, the motion simulation started with the humerus parallel to the ground, anterior to the scapular plane, and externally rotated and progressed by horizontally extending the humerus (i.e. rotating it posteriorly about an axis perpendicular to the transverse plane) into the position of apprehension (abducted and externally rotated posterior to the scapular plane) while maintaining the level of abduction and external rotation (Fig. 3C). To keep the joint articulated (i.e. maintain contact between the two bone's surfaces), a compressive force of 50N was applied to the centre of the humeral head, directed medially and maintained perpendicular to the glenoid face. This load was selected based on conditions employed in previous studies (Kaar et al. 2010, Walia et al. 2013) and pilot testing that showed no change in results for loads beyond

50N. The medial/lateral displacement of the centre of the humeral head and the angle of extension were recorded.

Outcome Variables & Statistical Analyses

The primary outcome variables were the rate of humeral head engagement on the anterior glenoid rim and the joint angle at which engagement occurred, termed the "engagement angle". The medial/lateral movement of the centre of the humeral head was recorded with respect to the angle of horizontal extension (Fig. 4), for both the intact humerus and all defect sizes. The medial/lateral positions of the humerus during simulations in the defect state, compared to the corresponding medial/lateral positions of the intact joint, were plotted with respect to joint angle. While engagement is conceptually simple, objective quantification proved to be difficult. A surgeon (G.S.A) observed simulated shoulder motion and indicated the moment at which defect engagement occurred (Fig. 5), and it was determined that this correlated to a medial displacement of the humeral head of 2mm in comparison to the normalized data plots for medial/lateral translation of the intact humeral head at that exact time. Thus, a medial translation of the humeral head ≥2mm was defined as the criterion for indicating engagement.

The occurrence of engagement (engagement or no engagement) was recorded at all defect sizes. A one-tailed McNemar test was performed for this outcome using SPSS software (SPSS Inc., Chicago, IL, USA) to assess marginal homogeneity. The engagement angle was quantified as the difference in joint angle between the scapular plane and the position when the humeral head engaged and dislocated. This outcome allowed for comparison between defect size and angle of engagement. Statistical analysis for this outcome consisted of a one-way repeated-measures analysis of variance (ANOVA) and pair-wise comparisons with a Bonferroni correction. All statistical measures defined significance as $p < 0.05$.

RESULTS

Glenohumeral Instability

The occurrence of HSD engagement was significantly different ($0.001<p<0.032$) between defect sizes (Fig. 6). All size XL and XXL HSDs engaged, 7 (58%) of the size L defects engaged, 2 (17%) of the size M defects engaged, and defect sizes XS and S did not engage the anterior glenoid rim. This resulted in a significant difference in instability between M vs. L defects ($p=0.032$), M vs. XL defects ($p=0.001$), and L vs. XL defects ($p=0.032$).

Joint Angle at Engagement

As HSD size increased, the magnitude of humeral extension range of motion to engagement (engagement angle) decreased, resulting in greater shoulder instability. The HSDs of size M, L, XL and XXL caused engagement at mean joint angles of -23.6±9.3°, -17.9±10.8°, -4.5±9.0°, and +6.4±8.8°, respectively (Fig. 7). These values were measured in relation to the scapular plane, where positive values represent engagement and dislocation anterior to the scapular plane and negative values are posterior to the plane. During simulated humeral extension, there were significant differences in the engagement angles between defect states ($p<0.001$). The size XXL HSDs engaged at a significantly lower engagement angle than size XL defects (10.9±1.2°, $p<0.001$) and size L defects (23.8±3.6°, $p<0.001$). The size XL defects engaged earlier than the size L defects (12.9±2.7°, $p<0.001$), and the size L defects engaged before the size M defects.

DISCUSSION

The influence of various HSD sizes on engagement and dislocation with shoulder motion in extension and rotation is not completely understood. The effect of anterior translation of the humerus on the glenoid has been examined (Kaar et al. 2010, Sekiya et al. 2009, Walia et al. 2013), however, there is no data that quantifies the independent effect of humeral extension on producing engagement in the defect state. This is important as it relates to the surgeons ability to examine for engagement intra-operatively with arthroscopy (Burkhart and De Beer, 2000). Intra-operatively while viewing through a posterior arthroscopic portal, instability can be revealed by translating the humeral head forward until dislocation or by placing the humeral head into abduction and external rotation and allowing the defect to rotate or horizontally extend to engagement. The translational method of determining engagement of a lesion may be less clinically relevant, as patients typically do not describe a recurrent dislocation occurring with an anteriorly directed force. Rather, most patients with recurrent instability describe apprehension or the occurrence of instability with the arm in abduction and external rotation(Taylor and Arciero, 1997). Therefore, our aim was to examine the role of range of motion, specifically humeral horizontal extension on engagement, independent from glenohumeral translation.

Our results indicated that glenohumeral joint translation is not necessarily required to produce instability when HSDs are present. With HSDs of at least 30% of the width of the humeral head (medium size defects), engagement and resultant dislocation occurred in 33 of 48 (69%) of the cases (12 specimens at 4 defect levels each). The presence of HSDs on the humeral head substantially reduces the arc length of the articular surface, resulting in engagement and dislocation. In the case of an intact humerus, the articular contact area is continuous throughout motion, whereas in the defect state the joint extends to an angle at which the leading edge of the defect moves anterior to the anterior glenoid rim. At this point the humeral head is no longer able to support the compressive articular load causing the humerus to medialize and engage on the glenoid rim (Miniaci A, 2004). This instability is important as it reveals that HSDs size M or larger are able to engage and result in dislocation even when the humeral head remains centered in the joint as it rotates. Therefore, patients with larger defects may be susceptible to engagement and dislocation while conducting simple joint rotations, without excessive forces or translations.

In the simulations of joint motion with HSDs of size XS and S (15% and 22.5% of the humeral head diameter), no joint dislocations were noted, and a dislocation rate of 16.7% was found for size M defects. This dislocation occurrence rate differed significantly from the large and extra-large defect states, as seen in Fig. 8. These results speak to the nature of translation and rotation in the interaction of a HSD on the glenoid rim. Anecdotic clinical experiences have demonstrated engagement with some extra-small and small lesions. This emphasizes that humeral translation or joint laxity may have some role to play in glenohumeral dislocation with smaller HSDs. This improves our understanding of the interaction between HSDs and the glenoid rim during in-vivo motion.

The glenohumeral joint angle at engagement produced further insight into the influence of HSD size on shoulder stability. An increase in HSD size had a direct effect on reducing the angle of extension at which engagement occurred. The average dislocation angle reduced from 23.6±9.3° posterior to the scapular plane to 6.4±8.8° anterior to the scapular plane as HSD size increased from M to XXL. The difference between engagement angles further emphasizes the significance of reducing the articular arc length of the humeral head. It is of particular interest to note that specimens with an extra-extra-large HSD engaged, on average, before even reaching the clinically apprehensive position in the scapular plane. As the humerus extended horizontally, the defect engaged at a mean angle of 6.4±8.8° anterior to the scapular plane. This finding is important as it reveals the high level of joint instability associated with very large HSDs. Thus, the results demonstrate that the shoulder joint is not required to approach end-range motion in order to cause instability. Furthermore, as these simulations were based on pure humeral rotation, it is possible that engagement would occur in even less extension if humeral translation and joint laxity was incorporated. This information also provides insight into whether a HSD will engage based on each patient's specific range of motion envelope. For example, some patients with normally less horizontal extension range of motion may not engage a larger HSD. This lack of engagement would occur because the patient's normal range of motion is less than the defect size-specific engagement angle. Conversely, some patients with greater than average horizontal extension motion may engage a smaller HSD. Additionally, not all specimens with a particular sized HSD engaged. For example, only 2 of 12 medium sized HSDs engaged (Fig. 8). This indicates that subtle differences in bony anatomy also have a role to play in instability. These differences may be accounted for through examining the effect of varying orientations of HSDs on the humeral articular surface, which is also likely to influence the interaction between the HSD and glenoid rim. In the case of this study, however, defect orientation was selected based on techniques used by Sekiya et al. (2009) and Yamamoto et al. (2007).

Some limitations were present in this in-silico biomechanical study. The models only included bony geometry of the joint with exclusion of cartilage and soft tissues. We elected not to model the anterior glenoid labrum, because it is typically detached and medialized after a shoulder dislocation. The study, however, is still effective in defining the influence of defect geometry on joint dislocation, which stands as the basis for when instability will occur. While HSDs have been shown to be associated with glenoid bone defects (Burkhart and Danaceau 2000, Burkhart and De Beer 2000, Sekiya et al. 2009, Yamamoto et al. 2007), we chose to focus solely on HSDs in order to examine their specific influence on joint stability. Defect depth was also modelled for a worst-case scenario, where the depth of the humeral defect extended to the humeral head/neck junction. While these worst-case defects occur clinically, patients may also present with shallower defects, and studies are underway to evaluate the effect of this variable. We do not view the constraining of humeral translation as a limitation. While this restriction may not fully replicate the in-vivo kinematics of the glenohumeral joint, it was imposed in order to study the effect of HSD size in isolation. As part of our future work we intend to evaluate mixed effects of humeral translation, defect orientation, and various joint motions. Examining more detailed depictions of shoulder rhythm is a further means of improving the efficacy of results.

CONCLUSIONS

Isolated glenohumeral joint rotation, without joint translation, results in Hill-Sachs defect engagement. The rate of engagement increased with defects >30.0% of the humeral head diameter, and defects smaller than that did not engage. Therefore, if these smaller Hill-Sachs defects clinically engage, we suspect that some degree of joint translation must be present. Additionally, as Hill-Sachs defects increased in size, the joint angle when engagement occurred significantly decreased.

ACKNOWLEDGEMENTS

The authors would like to acknowledge funding provided by the Natural Science and Engineering Research Council of Canada.

REFERENCES

Boileau P, Bicknell RT, El Fegoun AB, Chuinard C. 2007. Arthroscopic Bristow procedure for anterior instability in shoulders with a stretched or deficient capsule: the "belt-and-suspenders" operative technique and preliminary results. Arthroscopy 23: 593-601.

Boileau P, Villalba M, Hery JY, Balg F, Ahrens P, Neyton L. 2006. Risk factors for recurrence of shoulder instability after arthroscopic Bankart repair. J Bone Joint Surg Am 88: 1755-1763.

Burkhart SS, Danaceau SM. 2000. Articular arc length mismatch as a cause of failed bankart repair. Arthroscopy 16: 740-744.

Burkhart SS, De Beer JF. 2000. Traumatic glenohumeral bone defects and their relationship to failure of arthroscopic Bankart repairs: significance of the inverted-pear glenoid and the humeral engaging Hill-Sachs lesion. Arthroscopy 16: 677-694.

Calandra JJ, Baker CL, Uribe J. 1989. The incidence of Hill-Sachs lesions in initial anterior shoulder dislocations. Arthroscopy 5: 254-257.

Chen AL, Hunt SA, Hawkins RJ, Zuckerman JD. 2005. Management of bone loss associated with recurrent anterior glenohumeral instability. Am J Sports Med 33: 912-925.

Degen RM, Giles JW, Thompson SR, Litchfield RB, Athwal GS. 2013. Biomechanics of complex shoulder instability. Clin Sports Med 32: 625-636.

Giles JW, Elkinson I, Ferreira LM, Faber KJ, Boons H, Litchfield R, Johnson JA, Athwal GS. 2011. Moderate to large engaging Hill-Sachs defects: an in vitro biomechanical comparison of the remplissage procedure, allograft humeral head reconstruction, and partial resurfacing arthroplasty. J Shoulder Elbow Surg.

Hill HA, Sachs MD. 1940. The grooved defect of the humeral head. A frequently unrecongnized complication of dislocations of the shoulder joint. Radiology 35: 690-700.

Kaar SG, Fening SD, Jones MH, Colbrunn RW, Miniaci A. 2010. Effect of humeral head defect size on glenohumeral stability: a cadaveric study of simulated Hill-Sachs defects. Am J Sports Med 38: 594-599.

Kropf EJ, Sekiya JK. 2007. Osteoarticular allograft transplantation for large humeral head defects in glenohumeral instability. Arthroscopy 23: 322 e321-325.

McQuade KJ, Smidt GL. 1998. Dynamic scapulohumeral rhythm: the effects of external resistance during elevation of the arm in the scapular plane. J Orthop Sports Phys Ther 27: 125-133.

Miniaci A, G.M., 2004. Management of Anterior Glenohumeral Instability Associated With Large Hill–Sachs Defects. Tech. Shoulder Elb. Surg. 5, 170–175.

Re P, Gallo RA, Richmond JC. 2006. Transhumeral head plasty for large Hill-Sachs lesions. Arthroscopy 22: 798 e791-794.

Sekiya, J.K., Jolly, J., Debski, R.E., 2012. The Effect of a Hill-Sachs Defect on Glenohumeral Translations, In Situ Capsular Forces, and Bony Contact Forces. Am. J. Sports Med. 40, 388–394.

Sekiya JK, Wickwire AC, Stehle JH, Debski RE. 2009. Hill-Sachs defects and repair using osteoarticular allograft transplantation: biomechanical analysis using a joint compression model. Am J Sports Med 37: 2459-2466.

Taylor DC, Arciero RA. 1997. Pathologic changes associated with shoulder dislocations. Arthroscopic and physical examination findings in first-time, traumatic anterior dislocations. Am J Sports Med 25: 306-311.

Walia P, Miniaci A, Jones MH, Fening SD. 2013. Theoretical model of the effect of combined glenohumeral bone defects on anterior shoulder instability: a finite element approach. J Orthop Res 31: 601-607.

Wu, G., Van Der Helm, F.C.T., Veeger, H.E.J., Makhsous, M., Van Roy, P., Anglin, C., Nagels, J., Karduna, A.R., McQuade, K., Wang, X., Werner, F.W., Buchholz, B., 2005. ISB recommendation on definitions of joint coordinate systems of various joints for the reporting of human joint motion - Part II: Shoulder, elbow, wrist and hand. J. Biomech. 38, 981–992.

Yamamoto N, Itoi E, Abe H, Minagawa H, Seki N, Shimada Y, Okada K. 2007. Contact between the glenoid and the humeral head in abduction, external rotation, and horizontal extension: a new concept of glenoid track. J Shoulder Elbow Surg 16: 649-656.

Figure Legend

Figure 1 – Computer models of the humerus and scapula used during simulations, along with the glenoid coordinate system (A). In the position of apprehension, a line was drawn parallel to the anterior glenoid rim, representing the orientation of the Hill-Sachs defect on the humeral head (B). A Hill-Sachs defect created on the posterosuperior humeral head (C).

Figure 2 – Four points measuring the maximum superior/inferior length and anterior/posterior width of the glenoid rim were used to orient a coordinate system. The blue axis is perpendicular to the plane created by these four points, and was used to measure the medial/lateral movement of the humerus with respect to the glenoid during simulations.

Figure 3 – Positioning of the humerus with respect to the scapula to orient the model in the desired testing position. The simulation position included 90° of abduction, comprised of 60° of glenohumeral abduction and 30° of scapular elevation in the sagittal plane (A), 60° of humeral external rotation (B), and 60° of abduction in the anterior plane. From this position, the humerus was horizontally extended while maintaining the level of humeral abduction and external rotation (C).

Figure 4 – Normalized medial/lateral displacement data of the humerus for a shoulder specimen with different Hill-Sachs defect sizes. In cases of ≥2mm medial movement of the humeral head, the defect has engaged the anterior glenoid rim and the humeral head has dislocated medially. An angle of 0° corresponds to the humerus lying in the scapular plane.

Figure 5 – Computer simulation of horizontal humeral extension range of motion due to pure rotation with a 45.0% Hill-Sachs defect. Engagement is defined by ≥2mm medial movement of the humerus normalized to the intact condition. The figure illustrates 60 degrees of horizontal extension (A), 30 degrees of extension (B), pre-engagement (C) and engagement with dislocation (D).

Figure 6 – The occurrence of engagement for various sized Hill-Sachs defects. There was a significant increase in the number of 45.0% defects that engaged in comparison to the 37.5% defect (†: $p < 0.001$) and the 30.0% defect states (*: $p = 0.032$).

Figure 7 – Angle of humeral extension range of motion corresponding to Hill-Sachs defect engagement. Angles are in relation to the scapular plane, where positive° = anterior to plane, negative° = posterior to plane. The error bars represent 1 standard deviation. Differences in engagement angle between defect sizes were significant for all possible comparisons (*: $p < 0.001$).

Figure 8 – Percentage of dislocating Hill-Sachs defects at various joint angles. As Hill-Sachs defects increased in size, the angle of engagement decreased. Angles are in relation to the scapular plane, where positive° = anterior to plane, negative° = posterior to plane.

Figure 1
Click here to download Figure: Fig 1.pptx

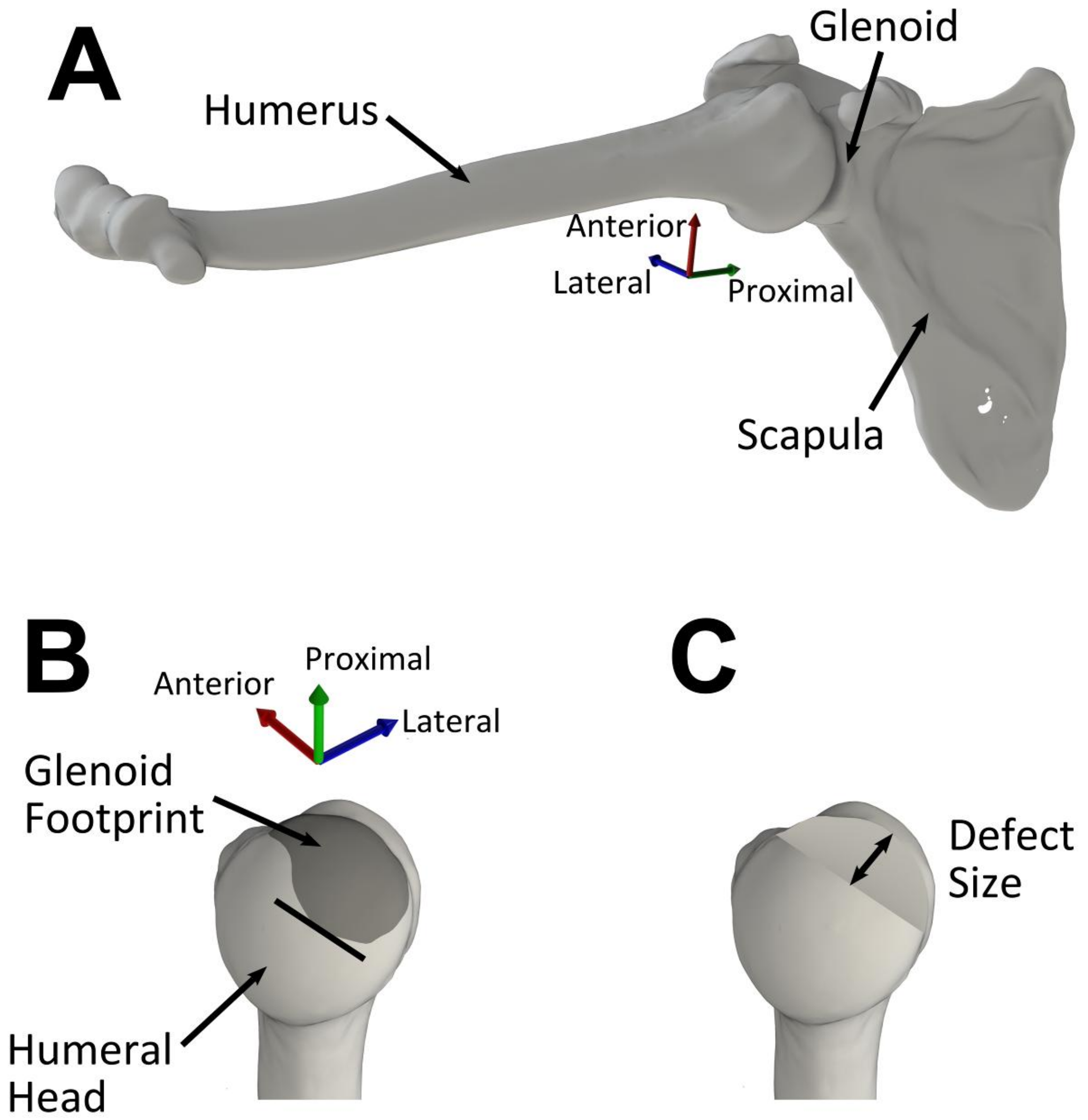

Figure 2

Click here to download Figure: Fig 2.pptx

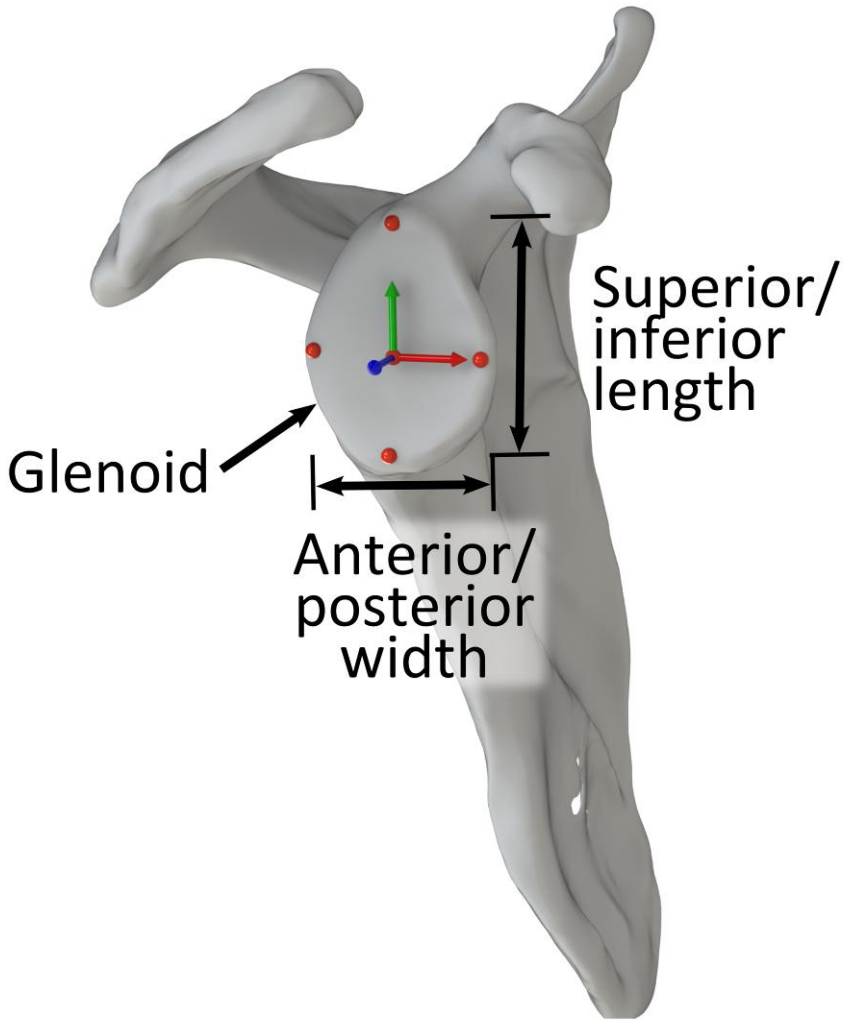

Figure 3
Click here to download Figure: Fig 3.pptx

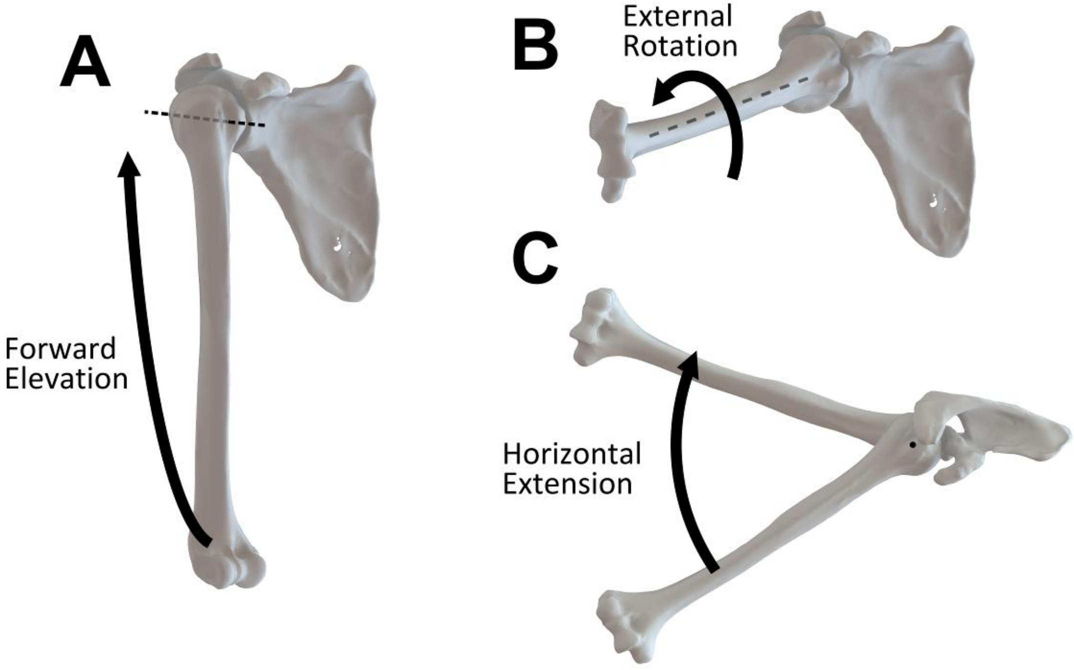

Figure 4

Click here to download Figure: Fig 4.pptx

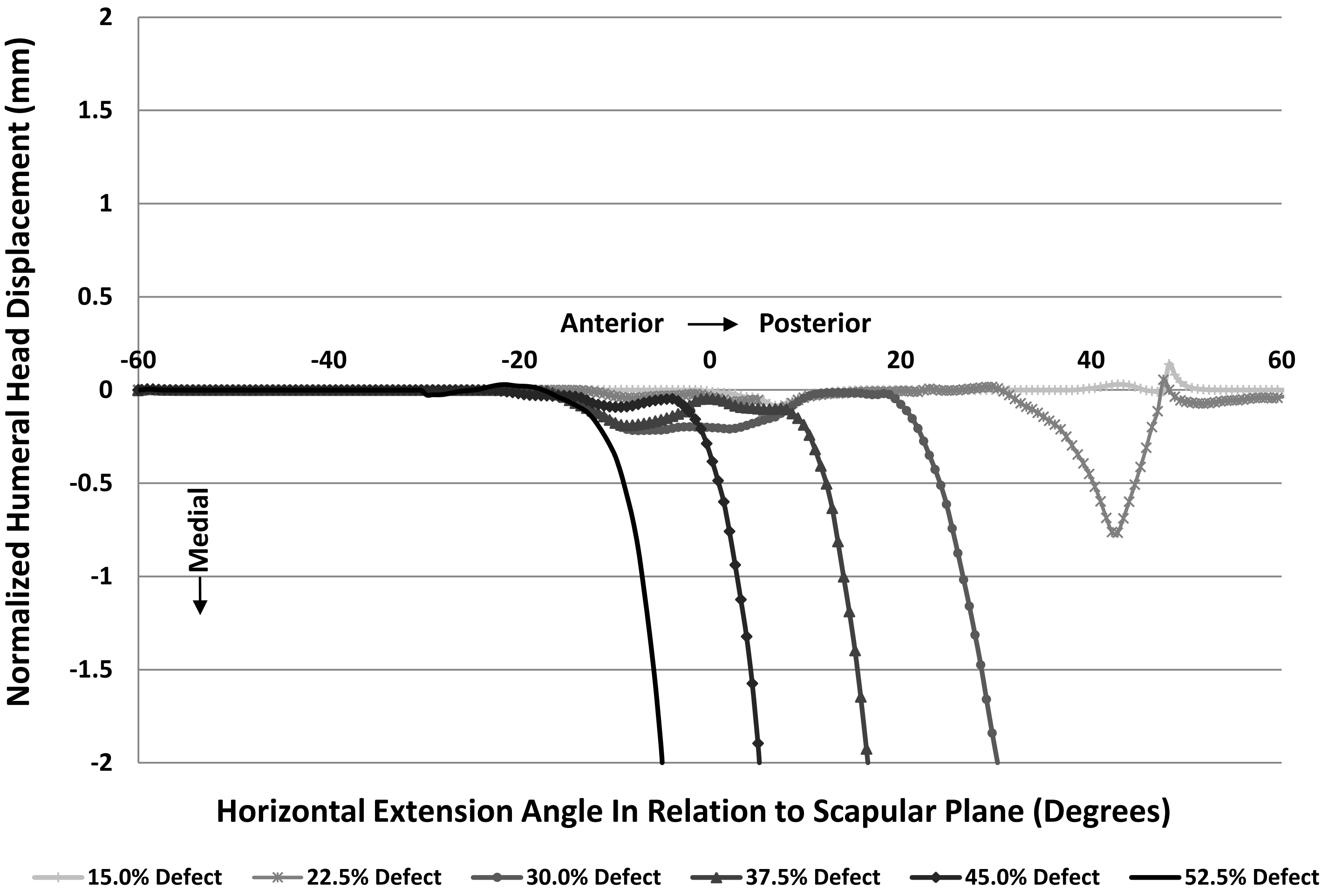

Figure 5

Click here to download Figure: Fig 5.pptx

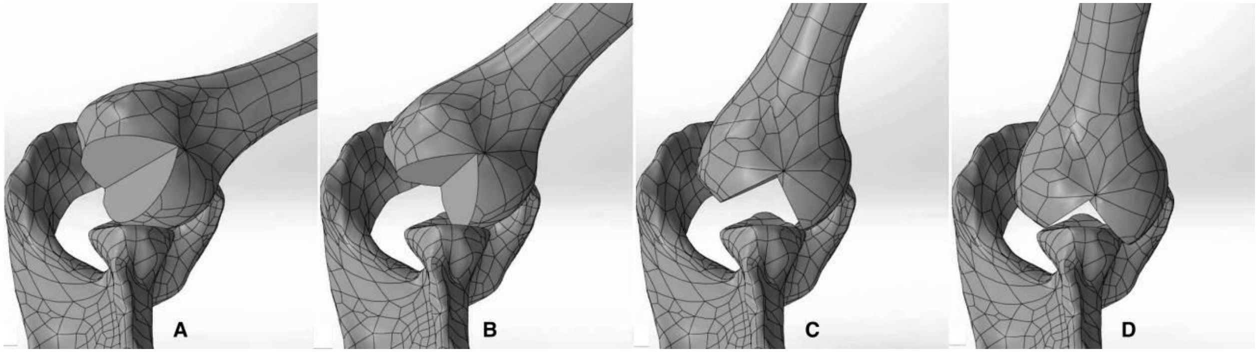

Figure 6
Click here to download Figure: Fig 6a.pptx

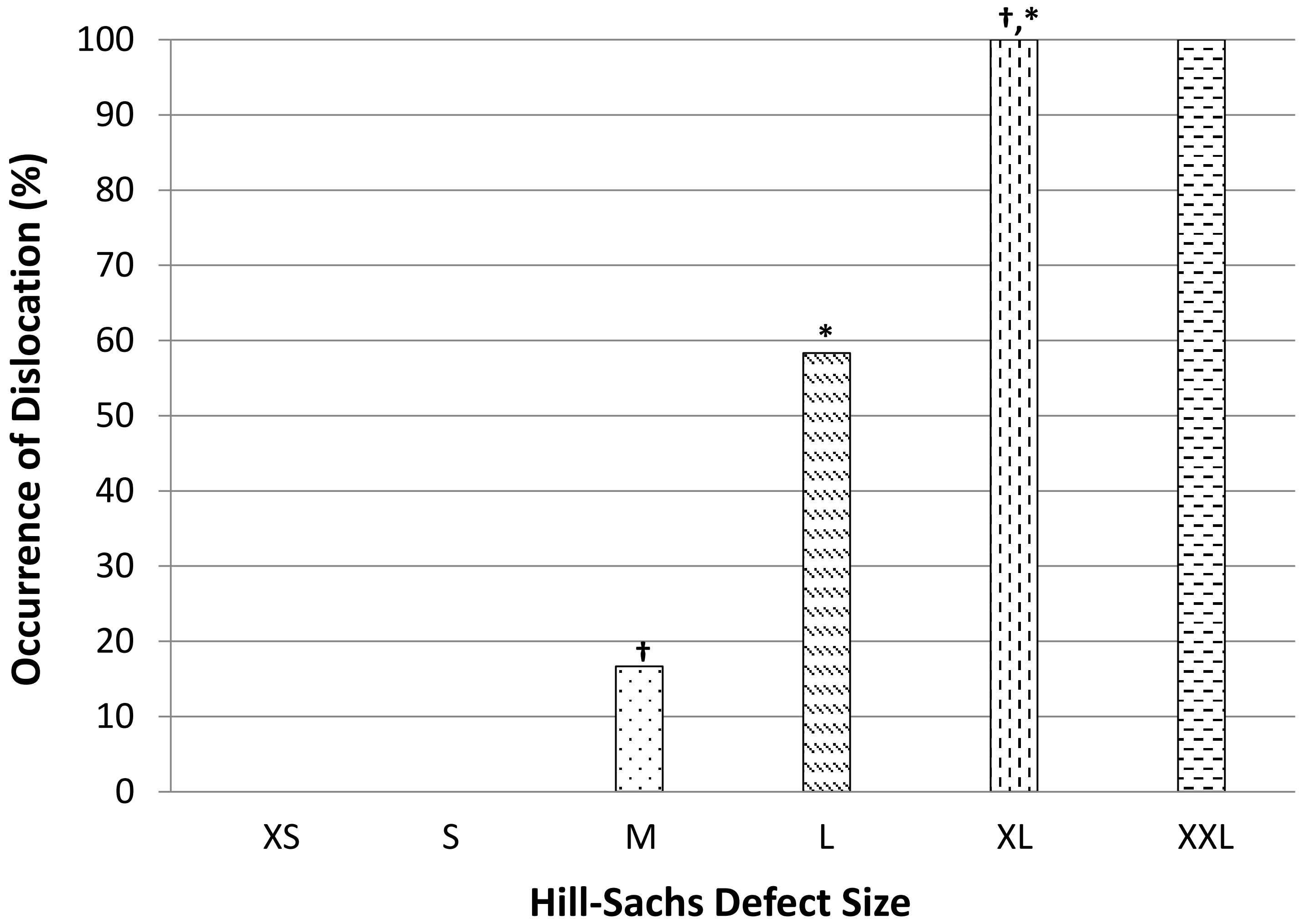

Figure 7
Click here to download Figure: Fig 7a.pptx

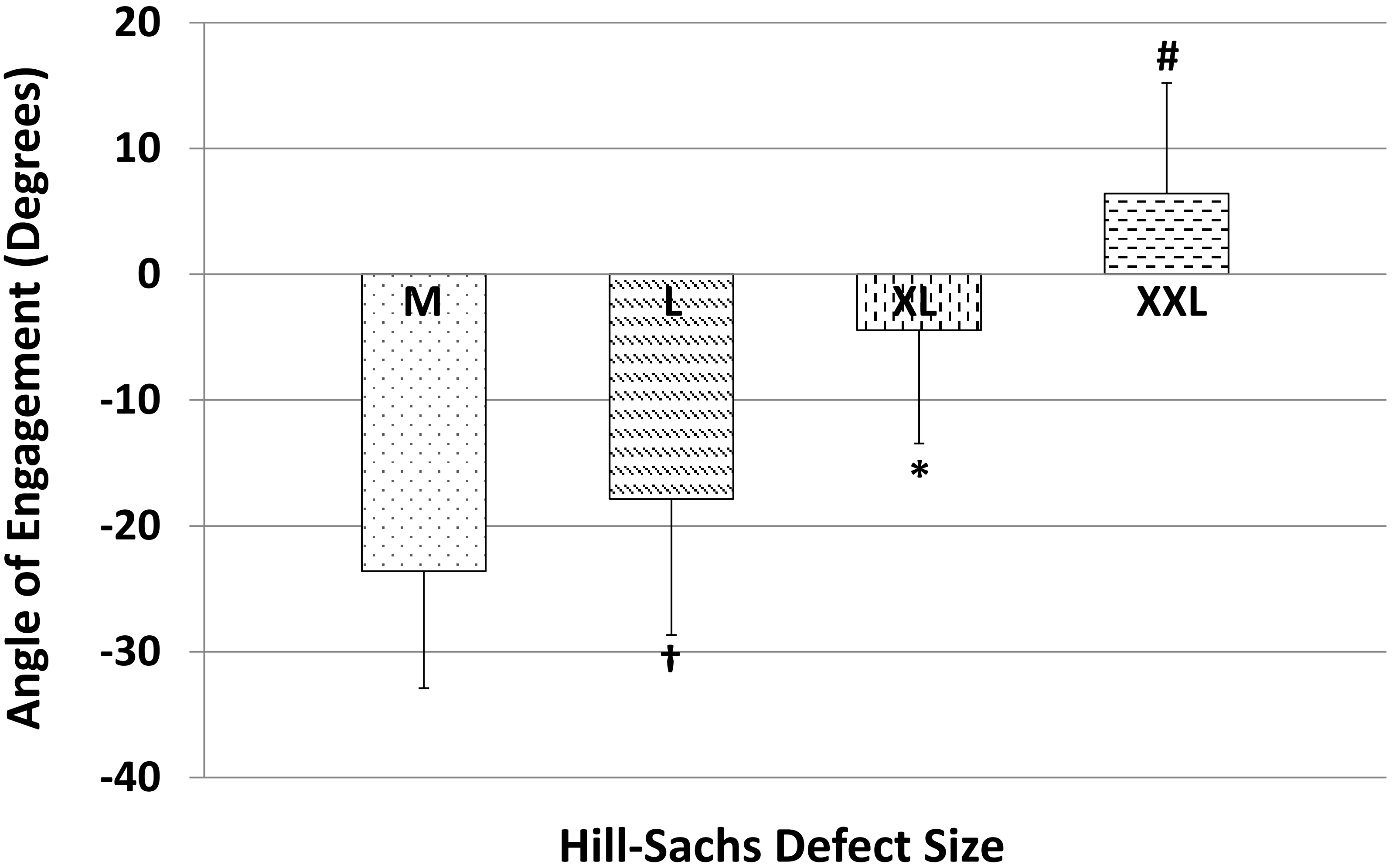

Figure 8
Click here to download Figure: Fig 8.pptx